# Development of High Throughput Glass Inkjet Devices for Pharmaceutical Applications

T. Ehtezazi[1,*], N. M. Dempster[1], G. D. Martin[2], S. D. Hoath[2], I. M. Hutchings[2]

[1] School of Pharmacy & Biomolecular Sciences, Liverpool John Moores University, Byrom Street, Liverpool, L3 3AF, UK

[2] Inkjet Research Centre, IfM, Department of Engineering, University of Cambridge, 17 Charles Babbage Road, Cambridge CB3 0FS, UK

## Abstract

The application of the inkjet method to pharmaceutical products is promising. To make this realistic, not only does the throughput of this method need to be increased, but also the components should be inert to pharmaceutical preparations. We present designs of glass based inkjet devices that are capable of producing droplets at high rates. To achieve this, inkjet devices from capillary tubes were manufactured with orifice diameters of 5µm, 10µm and 20µm and were actuated with diaphragm piezoelectric disks. Also, a pressure capsule was formed by creating a manifold at a distance from the orifice tip. Placing the piezoelectric disk at 0.5 mm distance from the tip allowed formation of a jet at 3.2MHz in certain designs, but for a short period of time due to overheating. The length of the pressure capsule, its inlet diameter and the nozzle tip geometry were crucial to lower the required power. Actuating an inkjet device with 10µm orifice diameter comfortably at 900 kHz and drying the droplets from 1% salbutamol sulphate solution allowed formation of particles with diameters of 1.76±0.15µm and the geometric standard deviation of 1.08. In conclusion, optimising internal design of glass inkjet devices allowed production of high throughput droplet ejectors.

Key words: Inkjet devices; high throughput; Pharmaceutical Inhalers; Spray drying; Uniform particles.

## Introduction

Inkjet printing methods have been utilised for pharmaceutical applications such as printing drug solutions on edible[1,2] and conventional papers[3,4] , manufacturing tablets[5-8], personalised medicine[9], preparation of bioadhesives[10], manufacture of spherical uniform particles[11,12] and manufacture of uniform and custom shape particles.[13]

However, the inkjet method has not been used in manufacture of pharmaceutical products at industrial scale or even small batch production. It appears the main reason has been the technical problems associated with the scale up of the inkjet method. For example, the droplet formation rate has been relatively slow. To overcome this limitation, novel inkjet devices have been developed that are capable of being actuated at 250 kHz[14], 890 kHz[15], 2.26 MHz[16], 2.30 MHz[17], and 2.80 MHz[18]. These achievements have increased the throughput of novel inkjet devices by about 100 times compared to conventional inkjet devices.

On the other hand, pharmaceutical regulations also require minimising the amount of impurities in pharmaceutical products.[19,20] Despite the progresses in the designs of inkjet devices, their applications could be questionable for pharmaceutical purposes. For example, the drug solution may contact directly with either the piezoelectric component,[16,18,20,21] or epoxy adhesive.[17] These arrangements may increase the level of impurities either in the drug substance or drug product. Furthermore, foreign particles must be identified and monitored in orally inhaled and nasal pharmaceutical products.[22] Therefore, if the components of an inkjet device were to decompose over time and shed particles, then meeting the above regulatory requirements would be challenging.

In this paper a general design of glass inkjet device is presented, which is capable of not only producing droplets at high frequencies, but also isolates the drug solution from other components such as epoxy adhesive, elastomers, metals or piezoelectric actuators. These glass inkjet devices would be more suitable for pharmaceutical applications, since the drug solution is in direct contact with glass, which is usually considered as an inert material. The inkjet devices were originally intended for producing respirable particles, but they may also be used for other pharmaceutical applications. In this work diaphragm piezoelectric devices were used due to their low cost, and thus more appropriate for multi-nozzles inkjet systems. "To improve the droplet generation of glass inkjet devices, a manifold was introduced at a distance before the inkjet device orifice. Then the dimensions and location of this manifold were optimised. "

## Material

Salbutamol sulphate was purchased from Bufa-Chemie (Castricum, The Netherlands). Acetone of analytical grade (AR) was purchased from Fisher Scientific (Loughborough, UK), and ethanol AR was obtained from Hayman (Essex, UK).

## Methods

### *Fabrication of Inkjet Devices*

The inkjet devices were manufactured in a similar manner to a previously reported method.[23] Briefly, the inkjet devices were made from 2 mm capillary tubes, and oxygen/propane flame

was used to create features in the tubes. Under controlled conditions, one end of the capillary tube was sealed by using the oxygen/propane flame. The preliminary observations indicated that to achieve a gradual collapse of the capillary tube, the intensity of the flame should not be high. This controlled fusion of the glass permitted formation of tapers inside the capillary tubes without shrinking the tube thickness. The tube was spun at 30 rpm by using an electromotor (Heidolph Schwabach, Germany) to ensure a uniform collapse. The same method was applied to make constrictions in the capillary tubes. All these manipulations were performed under a conventional field microscope (Nikon, Japan). The tip of the tube was ground to the taper using an in-house coarse grinder. This step was followed by a fine grinding process using optical fibre polishing papers (3M, LFG3P 3µm aluminium oxide, Thorlabs) to achieve the final desired orifice diameter. A hole was drilled at the centre of a diaphragm piezoelectric disk (Farnell, Leeds, UK) to accommodate the glass tube. A polypropylene tube with the internal diameter of 5 mm was cut to a desired length and placed on the piezoelectric disk with the help of the Blu-Tack adhesive (Bostik, Leicester, UK), a putty like pressure sensitive adhesive . The hole in the piezoelectric disk was in the centre of the propylene tube. The tip of the capillary tube was passed through the propylene tube and the hole in the piezoelectric disk, and the tip was allowed to protrude from the piezoelectric disk for a certain length such as 0.5 mm or 1 mm. A conventional epoxy resin adhesive was heated up to 70 ºC and used to fill the inside of the propylene tube to hold the piezoelectric disk and glass tube together. The heating of the adhesive not only allowed rapid curing of the glue, but also reduced the chance of air bubble formation in the adhesive. The presence of air bubbles not only resulted in unreliable jets, but also reduced the mechanical strength of the connection points. The presence of the polypropylene tube allowed the formation of reproducible epoxy resins columns on the piezoelectric disks. Figure 1A illustrates a schematic diagram of a typical in-house made inkjet device, and Figure 1B shows an image

of the glass capillary nozzle containing the taper, pressure capsule and constriction. Figure 1C presents a typical assembly of an inkjet device with reservoir.

***Droplet Formation***

The inkjet devices were actuated by a function generator (TG315, Thurlby Thandar Instruments, Huntingdon, UK) that was connected to an in-house amplifier. This system was capable of supplying signals with 30 V peak-to-peak amplitude and currents as high as 3 A. Double sided square waveforms were used, and the amplifier was capable of preserving the original shape of the waveform.

The inkjet devices were passed through a rubber septum and placed inside a vial (Figure 1C). Using a needle passed through the rubber septum, the air pressure inside the vial was adjusted. The inkjet devices ejected droplets in upwards direction that prevented nozzle blocking by falling particles onto the nozzle orifices. This configuration also prevented the contact of the drug solution with the rubber septum. Moreover, the preliminary work indicated that presence of a negative pressure at the tip of the nozzle was necessary to produce a jet at high frequencies. For example, the inversion of the inkjet device resulted in the dripping of the solution from the tip, and this prevented from jetting at high frequencies.

***Visualisation of Jets and Drops***

Shadowgraph imaging of the droplet streams used a 20 ns duration Nanolite spark flash light source and Ministrobokin power supply (High-Speed Photo-Système, Wedel, Germany) viewed by a x10 objective lens (Mitutoyo, Japan), telescope (Navitar Rochester, New York, USA) and CCD camera ( EC1020, Prosilica, USA). The CCD image pixel size (~ 1.1 μm) was calibrated offline with a 104 μm diameter wire. The generator bottle was clamped below the optical axis of the imaging system, with the orifice tip positioned near the optical focal plane at a distance of ~ 32 mm from the front of the objective lens. A micrometer adjusted the position of the optical telescope and CDD to bring the drop stream from the generator into focus for measurements of the droplets. The light source was fitted with a collimating lens and a thin diffuse plastic sheet to illuminate the region immediately above the nozzle and piezoelectric transducers droplet generator. Manual snapshots with a CCD exposure time of ~ 0.5 s and Ministrobokin internal triggering of ~ 2 Hz were recorded after initiating and visually checking the presence of droplet streams. Water was jetted throughout the visualisation work (at Cambridge). Several inkjet devices, with different nozzle orifice diameters, were tested. The average drop sizes and average spacing were determined by inspection of images using IrfanView (Irfan Skiljan, Austria) at each nozzle size and drive voltage, and drop spacing $\lambda$ and excitation frequency f imply average drop speed of $c = \lambda f$.

***Spray Drying System***

An inkjet device in the upright position was placed in the front of the drying chamber of a laboratory scale spray dryer, Buchi 190 (BÜCHI Labortechnik AG, Switzerland). A high performance cyclone was attached to the drying chamber and this itself was connected to a vacuum pump. The emitted droplets from the inkjet device were scattered into the drying chamber with the help of an air diffuser. The collection of particles in a container was

achieved by drawing air through the cyclone. This arrangement allowed spray drying at room temperature (approximately 20°C). The feed solutions contained at least 50% of organic solvents (acetone or ethanol). The solutions were filtered by a 0.2 µm PTFE filter (VWR, International) prior filling the reservoir, to remove particles.

***Scanning Electron Microscopy***

Spray dried particles were sputter coated with gold using an Emitech K550 (Ashford, UK) coater and then visualized with a Philips XL20 (Eindhoven, Holland) scanning electron microscope (SEM).

***Physical Particle Size Measurements***

The SEM images of particles were analysed for physical size measurements with the Scion Image Software, release Beta 3b (Scion Corporation, Maryland, USA). For each sample a minimum of 600 particles were analysed.

***Differential Scanning Calorimetry (DSC)***

DSC analyses were performed using a PerkinElmer DSC 8000 with Intracooler 2 cooling accessory and Pyris v. 10.1.0.0420 software (Seer Green, UK). The furnace temperature was calibrated using the Perkin Elmer supplied standard reference materials indium (m.p. = 156.60 °C) and zinc (m.p. =419.47 °C). Enthalpies of transition were calibrated with indium

with a heat of fusion ΔHf = 28.45 J $g^{-1}$. A sample (3–5 mg) was accurately weighed in crimped, standard aluminium pans and samples were held isothermally for 1 min at 25 °C before heating to 250 °C at 10 °C $min^{-1}$.

***Thermo-gravimetric Analysis***

Thermo-gravimetric analyses (TGA) were performed using a TGA7 with a TAC 7/DX Thermo Analysis Controller (Perkin Elmer, Bucks., U.K.) and Pyris software (PE, v. 3.81). Samples of 20 ± 2 mg were accurately weighed into a platinum boat and placed in the TGA furnace. The samples were heated from 25°C to 500°C at 10°C $min^{-1}$ in a nitrogen purged furnace (20 ml $min^{-1}$). Thermograms were produced by plotting the percent of sample weight against temperature. The percentage of mass loss calculated between 60°C and 140°C was attributed to moisture loss. Peaks representing the maximum rate of weight loss from first order derivative curves (d *%weight*/d*T*) were recorded as thermal decomposition temperatures ($T_d$ values) and used together with total % mass loss at the final temperature, for comparison of sample thermal degradation.

***X-ray powder diffraction (XRPD)***

The crystal behaviour of the samples were determined using a Rigaku Miniflex X-ray diffractometer (Osaka, Japan) calibrated using a silica standard plate. XRPD patterns were obtained using Cu Kα (1.54 Å) radiation, a voltage of 30 kV, and a current of 15 mA. Samples were prepared in 250 mm square zero background sample holders and analysed between 5and 40°2θ, with step increments of 0.02°2θ and scanning speed of2°2θ $min^{-1}$.

## Results

*Optimising the Design of Inkjet Devices*

Based on preliminary data an initial design of inkjet device was emerged with a manifold in the glass tube. Table 1 indicates the configurations of the inkjet devices to achieve droplet ejection at frequencies in the range of 360 to 800 kHz. The pressure capsule length was 11 mm, with the inlet (constriction) of 60 µm (tolerance of 10 µm). The piezoelectric disk was placed at a distance of 1 mm from the nozzle tip. The epoxy resin was placed inside a propylene tube with 13 mm length. Although high resonance frequencies were achieved, the diversity of frequencies was relatively wide considering similar dimensions of the inkjet devices used.

Table 2 presents the configurations of the inkjet device design with piezoelectric disk being positioned at 0.5 mm distance from the nozzle tip. Table 2 also shows that the length of epoxy resin tube (the propylene tube) was shortened to 3mm, and similarly the length of pressure capsule was reduced to 8mm. The length of epoxy resin tube was reduced to minimise the load on the piezoelectric disk. Therefore, small vibrations at high frequencies could be transferred efficiently to the glass tube. In Table 2, two orifice diameters are compared: 5 µm and 10 µm (both with the tolerance of 1 µm). It can be seen from Table 2 that not only high resonance frequencies were achieved, but also the frequency diversity was shorter (706.5 kHz to 886.0 kHz) compared to that in Table 1. In a few preliminary studies, the piezoelectric disk was positioned flush with the tip and high resonance frequencies were achieved similar to those in Table 2. However, on occasions, the leak of epoxy glue from the

piezoelectric disk, during device fabrication, caused permanent blockage of the nozzle orifice.

It is also evident from Table 2 that a low and consistent current (0.27 A) was sufficient to achieve a jet at a high frequency from inkjet devices with 5 µm orifice diameter. While, for inkjet devices with 10 µm orifice diameter not only the current was generally higher but also it was relatively inconsistent. High currents caused overheating of the inkjet device, which led to softening of the epoxy resin adhesive and also burning the piezoelectric component.

It should be noted that further reductions of the length of the pressure capsule were not helpful in achieving resonance frequencies with low and reproducible currents. Even, at pressure capsules with the length of 5 mm, the inkjet device failed to achieve a jet at any frequency.

Jets were prepared with resonance frequencies higher than those in Table 2 by reducing the inlet of the pressure capsule below 60 µm. This was more useful for inkjet devices with orifice diameters of 5 µm. However, extremely narrow inlets of pressure capsules caused occasional blockage of the inlet channel.

It was hypothesised that flow resistance at the nozzle orifice diameter could be one of the reasons for high currents required to achieve a jet at high frequencies. Therefore, in the following experiments the nozzle tip geometry was optimised by lowering the flow

resistance. This was achieved by preparing relatively abrupt tapers at the tip of the nozzle. To quantify this, the gap between the end of the glass capillary tube and the tip of the taper was measured prior to grinding the glass capillary tube. Figure 2 shows a schematic diagram of this arrangement.

Table 3 presents resonance frequencies of inkjet devices with controlled tip geometry. It can be seen that the gap between the end of the taper and the end of glass capillary tube (initial tip gap) varied between 320 µm and 500 µm. Preliminary studies showed that larger initial tip gaps resulted in orifice diameters starting from 20 µm. Table 3 indicates that not only high resonance frequencies were obtained in the range of 824.4 kHz to 925.2 kHz, but also the currents were low and in the range of 0.20 A to 0.27 A. The power consumption of the inkjet devices in Table 3 was in the range of 2.34 µJ to 6.11 µJ per droplet (with the assumption that a droplet was produced per device actuation or driving wave form).

It should be noted that all inkjet devices in Table 3 produced a jet at frequencies around 3.2 MHz (range: 3.29 MHz to 3.34 MHz), with currents in the range of 0.45 A to 0.78 A. However, these currents caused overheating of the inkjet device and consequently softening the adhesive (epoxy resin) which diminished the jet. Therefore, these frequencies could not be investigated further in detail using the existing design of inkjet devices.

*Droplet Speed and Diameter*

Figure 3 presents images of the droplets from inkjet devices with different orifice diameters and actuating at different frequencies. Figure 3A shows droplets that formed from an inkjet device with 20 µm orifice diameter at 334 kHz. This image reveals that although uniform

droplets were formed, the droplets merge further down from the device. Therefore, to prevent this, the droplets should be scattered as soon as they are formed.

Figure 3B and 3C show formation of uniform droplets from inkjet devices with 10 μm and 5 μm orifice diameters at 887 kHz and 849 kHz, respectively. However, for the inkjet device with 5 μm orifice diameter, although a jet formed at 885 kHz, it was not stable and occasionally irregular gaps were formed between the droplets (Figures 3D).

Table 4 shows the average droplet sizes and speeds from 3 different inkjet devices actuating in the range of 334 kHz to 885 kHz. In this table the results are also shown for an inkjet device with 20 μm orifice diameter with the chamber length of 15 mm and the constriction diameter of 130 μm.

Assuming that all the fluid ejects initially as a cylinder from the nozzle orifice of diameter D, and was observed as a stream of droplets (of diameter d) in the focal plane, $d = (3D^2\lambda/2)^{1/3}$ by conservation of fluid volume is independent of frequency (but depends on droplet spacing $\lambda$).

The observed droplet streams have drop spacing far below that of continuous inkjet (CIJ) systems, which typically require $\lambda \sim 5$ D. Generally for these inkjet devices $\lambda \sim 1.6$-2.2 D, far below the usual 5 D and the minimum spacing ($\lambda = \pi D$) required for Rayleigh break-up of a continuous jet. This implies that the droplet generation process cannot be that underlying conventional CIJ. However, the inkjet device with 5 μm orifice diameter at actuating frequency of 885 kHz had $\lambda$ of 5.4.

Table 4 indicates that droplet diameters were similar to the size of orifice diameters for inkjet devoices with 20 µm and 10 µm orifice diameters. However, for the 5 µm orifice diameter, the droplet diameters were greater than the nozzle diameter. The droplet speed was in the range of 9 to 19 m/s, however, this was increased to 32 m/s for the inkjet device with 5µm orifice diameter at 885 kHz actuating frequency. In addition, Table 4 shows that reducing current and voltage not only reduced droplet diameter, but also the droplet velocity. Images of droplets showed droplet merge further down the nozzle tip at these actuating parameters.

*Morphology of Produced Particles*

Table 5 shows the geometric standard deviation (GSD) and diameter of particles produced by the inkjet spray drying system using inkjet devices with geometries indicated in Table 3. In Table 5, feed rate presents the volume of a solution that was sprayed in average over an hour by the inkjet device. In these experiments organic solvents were added to the feed solution to ensure rapid drying of droplets. The cooling effects of the air diffuser prevented overheating of these inkjet devices.

It can be seen from Table 5 that the GSD of produced particles was in the range of 1.06 to 1.09. A typical SEM image of particles is illustrated in Figure 4A, when acetone was the organic solvent. The uniformity of particles is evident from this image and suggests uniform droplets were produced from inkjet devices at high resonance frequencies.

Figure 4B shows particles that were produced from a solution that contained ethanol as organic solvent (3.3% w/v solution in Table 5). It can be seen that particles contained dimples as structural features. In addition, the particles not only had similar diameters, but also most of them had the same size dimples with mostly containing singular dimple. This observation indicates that changing solvent in spray drying system may add extra features into the produced particles, and if all droplets have the same size; and the drying conditions for them are identical, then produced particles would have the same additional feature with the same size.

***Solid State Properties***

To obtain sufficient amounts of powder for the purpose of solid state characterisation, the inkjet device with 20 µm orifice diameter (stated in the above) was utilised to produce particles at 350 kHz with the feed solution of 1% of salbutamol sulphate, which contained 50% acetone. The produced particles had size of 5.28 ± 1.16 µm with the GSD of 1.29. The efficiency of the spray drying system was 40% for this size of particles.

*The DSC observations*

Figure 5 shows the DSC diagram of particles made by the 20 µm inkjet device. No-distinct melting endotherm peak was observed from the spray dried material, however, the DSC curve showed a broad endotherm peak between 50-110$^{o}$C and irregular noise above 160$^{o}$C, indicative of moisture loss and sample breakdown, respectively.

Figure 5 also illustrates the DSC diagram of the original salbutamol sulphate powder which showed no evidence of moisture loss but did exhibit a distinct endotherm, characteristic of crystal melting (extrapolated onset 178$^{o}$C).

*The TGA Observations*

Figure 6 shows the TGA diagram of particles prepared by the 20 µm inkjet device. It is evident that powder contained approximately 1% moisture and initial degradation of the sample was apparent above 170$^{o}$C. The total mass loss for the spray dried salbutamol sample was 48.5% at 500$^{o}$C and Td values were obtained from four peak apices on the first derivative curve; Td1=102$^{o}$C, Td2=189$^{o}$C, Td 3= 257$^{o}$C and Td4=355$^{o}$C. Figure 6 also illustrates the TGA diagram of the original powder, which showed no evidence of sample degradation below 225$^{o}$C and less than 0.1% moisture content. The total mass loss at 500$^{o}$C was calculated as 51% and Td values were obtained from only two peak apices on the first derivative curve; Td1=270$^{o}$C and Td 2= 362$^{o}$C.

*The XRPD Observations*

XRPD diagrams from the original salbutamol sulphate powder and particles prepared by the 20 µm inkjet device are presented in Figure 7. The crystalline nature of the original drug was clearly demonstrated by its characteristic XRPD pattern containing well defined peaks between 22° to 40°2 theta. In contrast, the inkjet spray dried drug was found to contain only amorphous particles indicating that the crystalline nature of the product was not formed during the spray drying process.

## Discussion

This study demonstrated a design of glass inkjet devices achieving high frequencies comfortably around 800 kHz. The inkjet devices were based on the squeeze mode design and produced uniform droplets at these high frequencies. The inkjet devices in this study produced droplets at rates of 100 times more than conventional inkjet devices.[24-27]The improved performances of inkjet devices may be partly attributed to the presence of a constriction in the capillary tube. The incorporation of a manifold has been reported previously in the design of inkjet devices.[28-30]

Our observations showed that droplet diameter was greater than the orifice diameter for inkjet devices with 5 µm orifice diameter. These observations suggest that the viscous effects of the feed solution might have resulted in building up a pressure inside the pressure chambers of the 5µm inkjet devices. Therefore, in the droplet ejection process, more of the liquid protruded from the device and consequently the volume of the emitted droplet increased. However, for inkjet devices with 10 µm and 20 µm orifice diameters, the droplet diameters were less than the orifice diameters. A previous study also demonstrated production of droplets smaller than the inkjet orifice diameter at high frequencies. These devices also had 10 µm orifice diameters and were actuated at frequencies in the range of 470 kHz to 2.26 MHz.[16]

The inkjet devices in our study were actuated in an inverted position, which is not common. This arrangement prevented contact of the feed solution with the rubber part of the solution

reservoir. Therefore, the feed solution was in contact with glass compartments at all the time. As a result, the risk of increasing the level of impurities (leachables and extractables) would be eliminated in the emitted droplets or particles produced in an inkjet spray drying system.

Inkjet heads have been developed by applying micro-electro-mechanical systems (MEMS) methods.[16-18, 29-32] However, overheating was reported for an inkjet head at 980 kHz.[31]On the contrary, our inkjet devices achieved resonance frequencies around 800 kHz without significant over-heating. The power consumption in our devices was in the range of 2.34 µJ to 6.11 µJ to produce one droplet per nozzle. These are much greater than previous observations.[32] The main reason is that the previous inkjet head contained arrays of ejectors, while in our study only a single ejector was assigned to a single piezoelectric disk.

To overcome the overheating problem, a nebuliser has been developed based on the Fourier horn resonators.[33] This device ejected droplets with the help of a piezoelectric transducer at frequencies in the range of 0.28-1.46 MHz. The mechanism of droplet generation was based on the vibration of a thin layer of the nebulising solution at the tip of the device. At the resonance frequency of 961 kHz, the flow rate of nebulising solution was 300 µl/min (or 18 ml/hour), which is much greater than our inkjet devices. The power requirement for atomisation was 0.25 W at 961 kHz, which is much less than our inkjet devices. However, this nebuliser was extremely sensitive to fluctuations of the actuating frequency and only 1 kHz deviation from the resonance frequency was sufficient to cease droplet generation. Furthermore, due to the nature of the droplet generation, the droplets were not as uniform as droplets produced by the inkjet devices in our study.

In an alternative approach, a nebuliser was developed based on the vibrating mesh mechanism.[34] The orifice diameter was 4µm and the device was operated at 127 kHz. The vibrating mesh contained microactuators with conical shape, and the inlet was 80 µm. The nozzles were made in a silicon wafer with the number of 14,000 nozzles per $cm.^2$ However, the droplets produced were not uniform and the size distribution was stretched from 1µm to 50µm. This observation could be due to the breaking of droplets into several smaller droplets with different sizes, while emitting from the nozzles.

It should be noted that the scale-up of the glass inkjet devices faces challenges. This is mostly due to manual processing of each inkjet device. Therefore, if glass inkjet devices are considered for use at industrial scale, two main improvements should be achieved. First, the manufacture of glass inkjet devices should be automated; second, the droplet formation rate of inkjet devices should be increased even further. This would result in less inkjet devices to be included in an industrial inkjet head.

In this paper, the solid state characterisation methods identified formation of amorphous particles from the inkjet spray drying system and this is similar to a previous work.[35]In addition, the moisture contents were similar for inkjet spray dried particles and a conventional method.[35] However, the inlet temperature in the previous study was 150 °C, and in our inkjet spray drier it was room temperature. It should be noted that the feed solution in our study contained acetone which helped drying droplets at room temperature.

## Conclusions

This study employed designs of glass inkjet devices that produced uniform particles at high frequencies in the range of 800-900 kHz. Key design parameters were: the presence of a constriction (manifold), proximity of piezoelectric disk to the orifice, and nozzle tip geometry with low flow resistance. The power consumption of inkjet devices was low enough to actuate them for a long period of time. The arrangements of components in the inkjet devices made these devices less susceptible to addition of impurities to the product.

## Conflict of Interest

There is no conflict of interest.

## List of Figures

**Figure 1.** A) Schematic diagram of the in-house-made inkjet device. B) An image of the glass part of an inkjet device, presenting the pressure capsule, the constriction before the pressure capsule (inlet) and the nozzle tip (the orifice). C) A typical assembly of a glass inkjet device with reservoir.

**Figure 2.** Schematic diagram of the glass tip before grinding, illustrating the tip geometry identified in the inkjet devices.

**Figure 3.** Images of droplets produced by inkjet devices**.** A) Orifice diameter of 20 μm at 334.5 kHz, droplet merge further down the tip is indicated by an arrow. B) Orifice diameter of 10 μm at 887 kHz. C) Orifice diameter of 5 μm at 849 kHz. D) Orifice diameter of 5 μm at 885 kHz.

**Figure 4.** SEM images of particles produced by the inkjet device P at high frequencies in the spray drying system. A) Particles produced at 901.4 kHz frequency with 1% salbutamol sulphate solution which contained acetone (50% V/V). B) Particles produced at 838.6 kHz frequency with 3.3% salbutamol sulphate solution which contained ethanol (70% V/V). The characteristics of the inkjet device P are depicted in Table 3.

**Figure 5.** Comparison of DSC thermograms from inkjet spray dried and original bulk salbutamol sulphate particles.

**Figure 6.** Comparison of thermograms from TGA of inkjet spray dried and original bulk salbutamol sulphate particles.

**Figure 7.** Comparison of X-ray powder diffractograms from inkjet spray dried and original bulk salbutamol sulphate particles.

## References


1. Buanz AB, Saunders MH, Basit AW, Gaisford S 2011. Preparation of personalized-dose salbutamol sulphate oral films with thermal ink-jet printing. Pharm Res 28:2386-2392.

2. Raijada D, Genina N, Fors D, Wisaeus E, Peltonen J, Rantanen J, Sandler N 2013. A Step Toward Development of Printable Dosage Forms for Poorly Soluble Drugs. JPharm Sci102:3694-3704.

3. Sandler N, Määttänen A, Ihalainen P, Kronberg L, Meierjohann A, Viitala T,Peltonen J 2011.Inkjet printing of drug substances and use of porous substrates-towards individualized dosing. J Pharm Sci 100:3386-3395.

4. Genina N, Fors D, Vakili H, Ihalainen P, Pohjala L, Ehlers H, Kassamakov I,Haeggström E, Vuorela P, Peltonen J, Sandler N 2012. Tailoring controlled-release oral dosage forms by combining inkjet andflexographic printing techniques.Eur J Pharm Sci47:615-623.

5. Wu BM, Borland SW, Giordano RA, Cima LG, Sachs EM, Cima MJ 1996. Solid free-form fabrication of drug delivery devices. Journal of Control Release 40:77-87.

6. Katstra WE, Palazzolo RD, Rowe CW, Giritlioglu B, Teung P, Cima MJ 2000. Oral dosage forms fabricated by Three Dimensional Printing™. Journal of Control Release 66:1-9.

7. Rowe CW, Katstra WE, Palazzolo RD, Giritlioglu B, Teung P, Cima MJ 2000. Multimechanism oral dosage forms fabricated by three dimensional printing. J Control Release 66:11-7.

8. Lam CXF, Mo XM, Teoh SH, Hutmacher DW 2002. Scaffold development using 3D printing with a starch-based polymer. Materials Science and Engineering C 20:49-56.

9. Scoutaris N, Alexander MR, Gellert PR, Roberts CJ 2011. Inkjet printing as a novel medicine formulation technique. J Control Release 156:179-185.

10. Doraiswamy A, Dunaway TM, Wilker JJ, Narayan RJ 2009. Inkjet printing of bioadhesives. J Biomed Mater Res B Appl Biomater 89:28-35.

11. Iwanaga S, Saito N, Sanae H, Nakamura M 2013. Facile fabrication of uniform size-controlled microparticles and potentiality for tandem drug delivery system of micro/nanoparticles. Colloids and Surfaces B: Biointerfaces 109:301-306.

12. Ehtezazi T, Davies MJ, Seton L, Morgan MN, Ross S, Martin GD, Hutchings IM 2014. Optimizing the primary particle size distributions of pressurized metered dose inhalers by using inkjet spray drying for targeting desired regions of the lungs. Drug Dev Ind Pharm Nov 19. [Epub ahead of print] PubMed PMID: 24252108.

13. Lee BK, Yun YH, Choi JS, Choi YC, Kim JD, Cho YW 2012. Fabrication of drug-loaded polymer microparticles with arbitrary geometries using a piezoelectric inkjet printing system. Int J Pharm 427:305-310.

14. de Heij B, van der Schoot B, Bo Hu, Hess J, de Rooij NF 2000. Characterisation of afL droplet generator for inhalation drug therapy, Sensors and Actuators A: Physical 85:430-434.

15. Forbes TP, Degertekin FL, Fedorov AG 2007. Multiplexed operation of a micromachined ultrasonic droplet ejector array. Rev Sci Instrum 78:104101 (1-6).

16. Demirci U, Yaralioglu GG, Hæggström E, Percin G, Ergun S, Khuri-Yakub BT 2004. Acoustically actuated flextensional $Si_xN_y$ and single-crystal silicon 2-D micromachined ejector arrays. IEEE Transactions on Semiconductor Manufacturing17:517-524.

17. Meacham JM, Ejimofor C, Kumar S, Degertekin FL, Fedorov AG 2004. Micromachined ultrasonic droplet generator based on a liquid horn structure. Rev Sci Instrum 75:1347-1352.

18. Percin G, Khuri-Yakub BT 2002. Piezoelectrically actuated flextensionalmicomachined ultrasound droplet ejectors. IEEE Transactions on Ultrasonics, Ferroelectrics, and Frequency Control 49:756-766.

19. International Conference on Harmonisation, ICH Q8 (R2) Pharmaceutical Development 2009 Step 4 version.

20. Pilaniya K, Chandrawanshi HK, Pilaniya U, Manchandani P, Jain P, Singh N 2010. Recent trends in the impurity profile of pharmaceuticals. J Adv Pharm Technol Res 1:302-310.

21. Sangplung S, Liburdy JA 2009. Droplet formation under the effect of a flexible nozzle plate. Journal of Colloid and Interface Sci 337:145-154.

22. Nagao LM, Lyapustina S, Munos MK, Capizzi MD 2005. Aspects of particle science and regulation in pharmaceutical inhalation drug products. Crystal Growth & Design 5:2261-2267.

23. Lee E.R 2002. Microdrop Generation. Series Editor: Sergey Edward Lyshevski. CRC Press pp 115-173.

24. Bogy DB, Talke FE 1984. Experimental and theoretical study of wave propagation phenomena in drop-on-demand ink jet devices. IBM J Res Develop 28:314–321.

25. Yoon YK, Park JH, Lee JW, Prausnitz MR, Allen MG 2011. A thermal microjet system with tapered micronozzles fabricated by inclined UV lithography for transdermal drug delivery. J Micromechan Microeng 21:025014-025022.

26. Reis N, Ainsley C, Derby B 2005. Ink-jet delivery of particle suspensions by piezoelectric droplet ejectors J Appl Phys 97:094903_1-094903_6.

27. Wijshoff H 2010. The dynamics of the piezo inkjet print-head operation. Physics Reports 491:77-177.

28. Yang JC, Chien W, King M, Grosshandler WL 1977. A simple piezoelectric droplet generator. Experiments in Fluids 23:445-447.

29. Kim CS, Park SJ, Sim W, Kim YJ, Yoo Y 2009. Modeling and characterization of an industrial inkjet head for micro-patterning on printed circuit boards. Computers & Fluids 38:602-612.

30. Kim CS, Sim W, Lee JS, Yoo Y, Joung J 2010. Design and characterization of piezoelectric inkjet for micro patterning of printed electronics IEEE 1817-1822.

31. Zarnitsyn VG, Meacham JM, Varady MJ, Hao C, Degertekin FL, Fedorov AG 2008. Electrosonic ejector microarray for drug and gene delivery. Biomed Microdevices 10:299-308.

32. Demirci U, Yaralioglu GG, Haeggstrom E, Khuri-Yakub BT 2005. Femtoliter to picoliter droplet generation for organic polymer deposition using single reservoir ejector arrays. IEEE Trans Semi Man18:709–715.

33. Tsai SC, Cheng CH, Wang N, Song YL, Lee CT, Tsai CS 2009. Silicon-based megahertz ultrasonic nozzles for production of mono-disperse micrometer-sized droplets. IEEE Trans Ultrason Ferroelectr Freq Control 56:1968-1979.

34. Shen SC 2010. A new cymbal-shaped high power microactuator for nebulizer application. Microelec Eng 87:89-97.

35. Columbano A, Buckton G, Wikeley P 2002. A study of the crystallisation of amorphous salbutamol sulphate using water vapour sorption and near infrared spectroscopy. Int J Pharm 237:171-178.

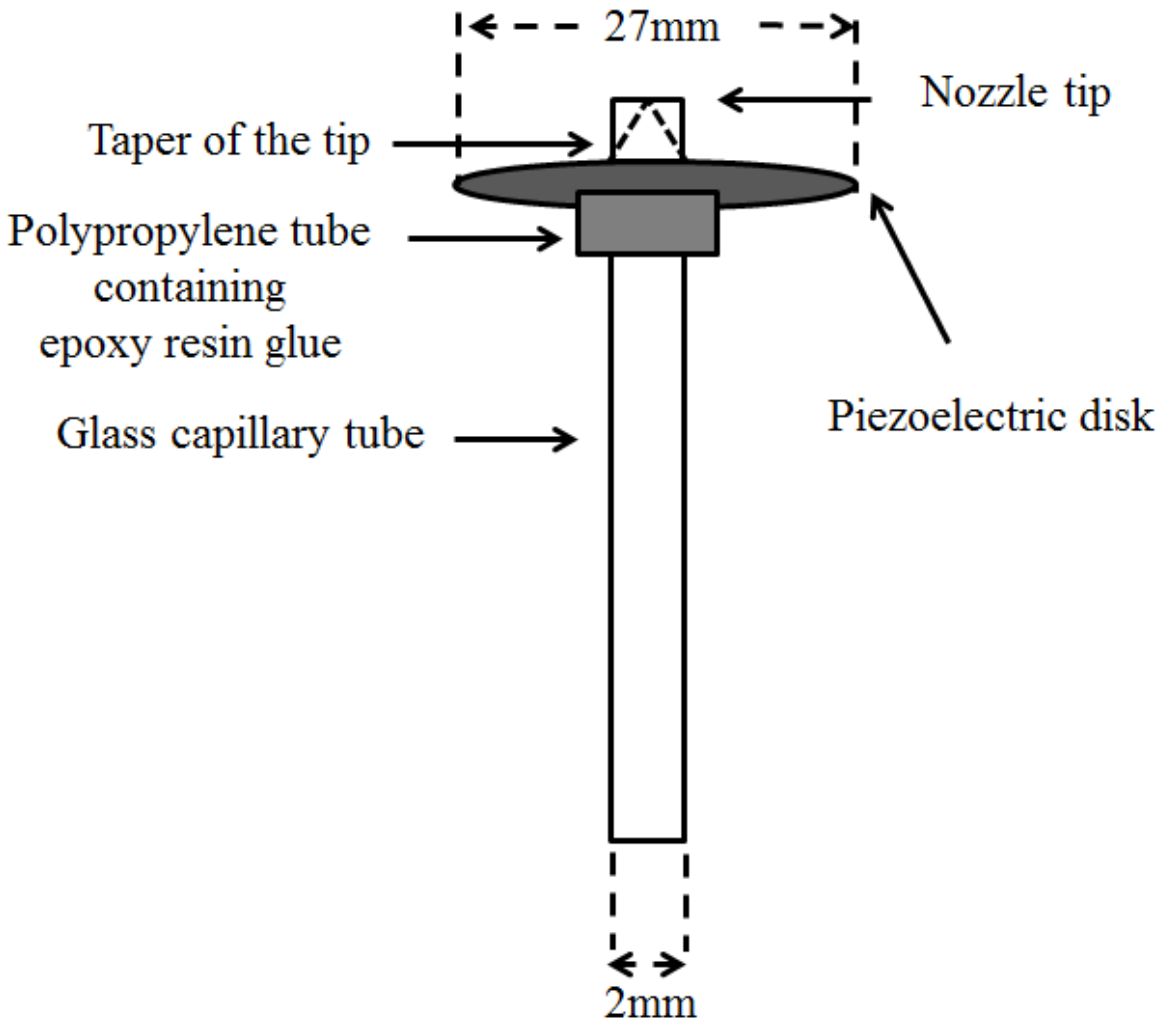
27mm
Nozzle tip
Taper of the tip
Polypropylene tube
containing
epoxy resin glue
Glass capillary tube
Piezoelectric disk
2mm

Figure 1A

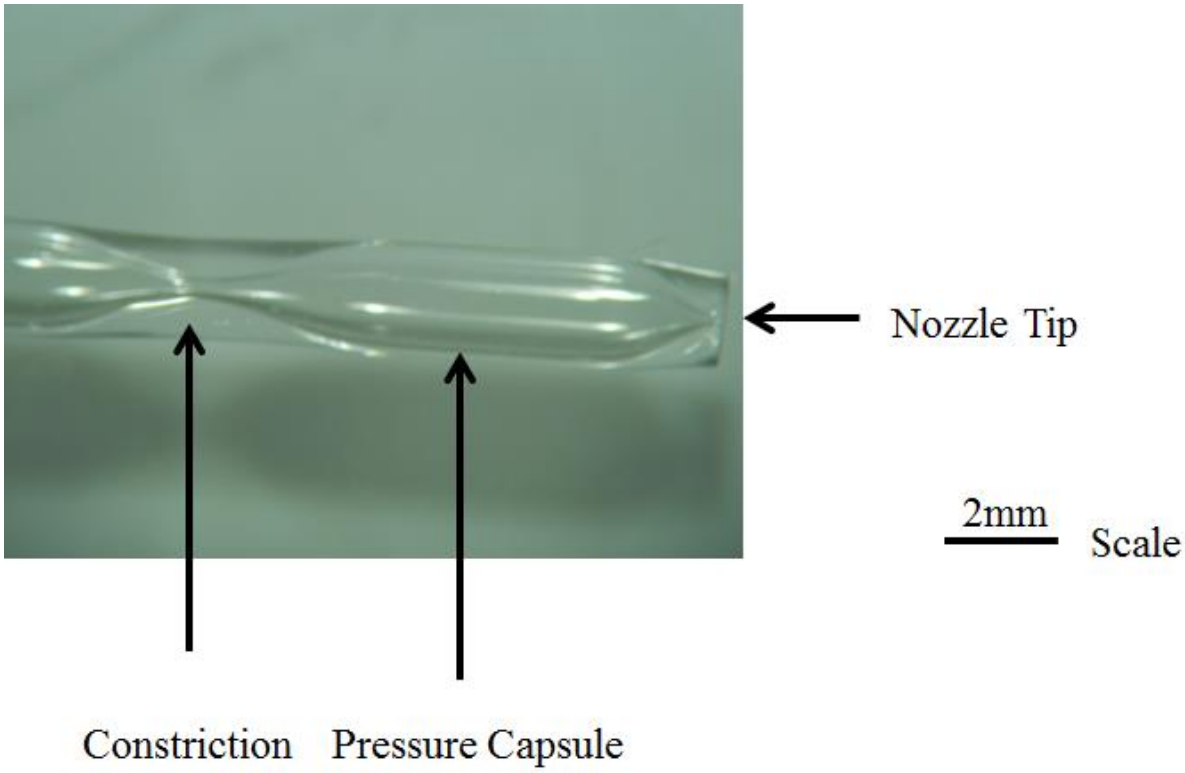


Figure 1B

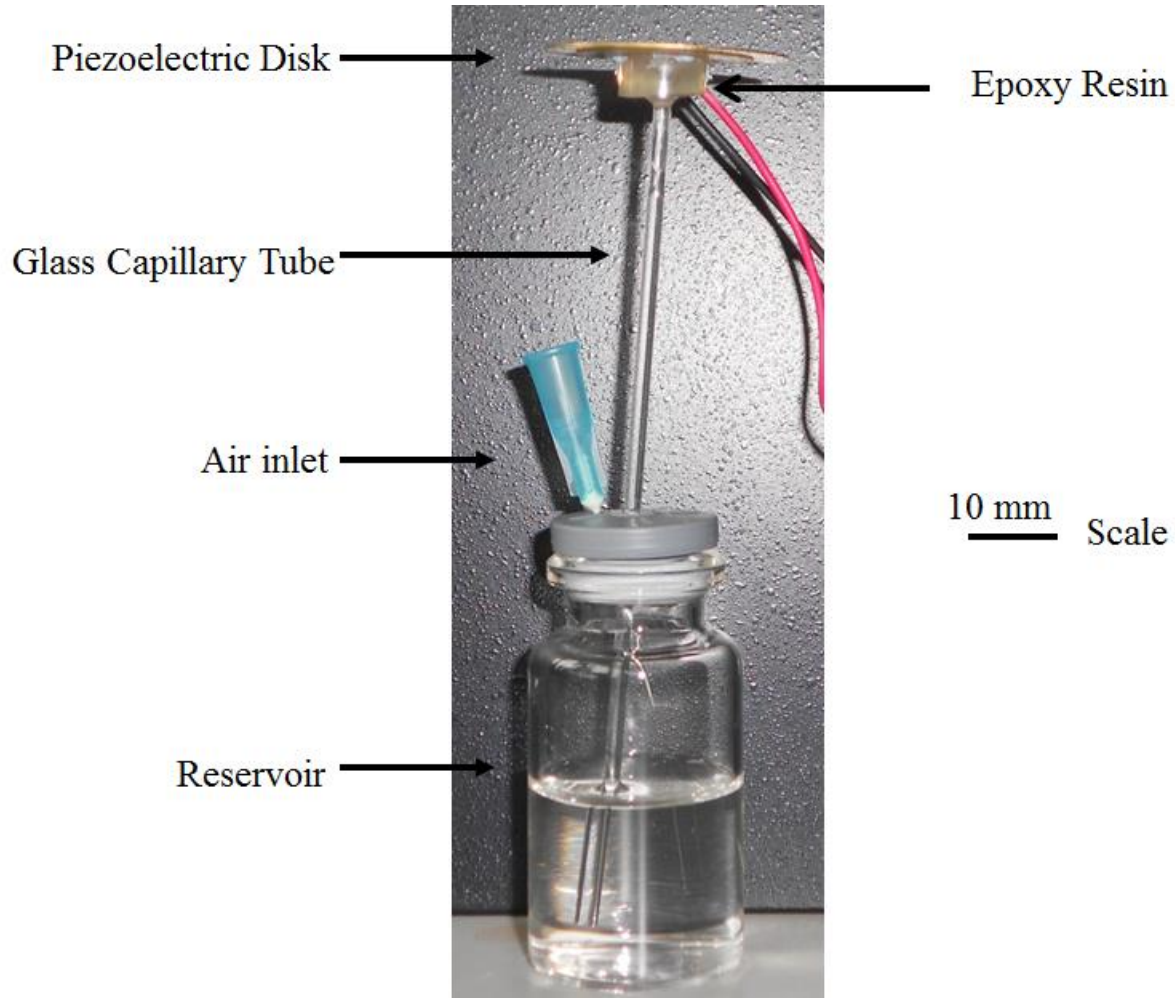
Piezoelectric Disk
Epoxy Resin
Glass Capillary Tube
Air inlet
10 mm
Scale
Reservoir

Figure 1C

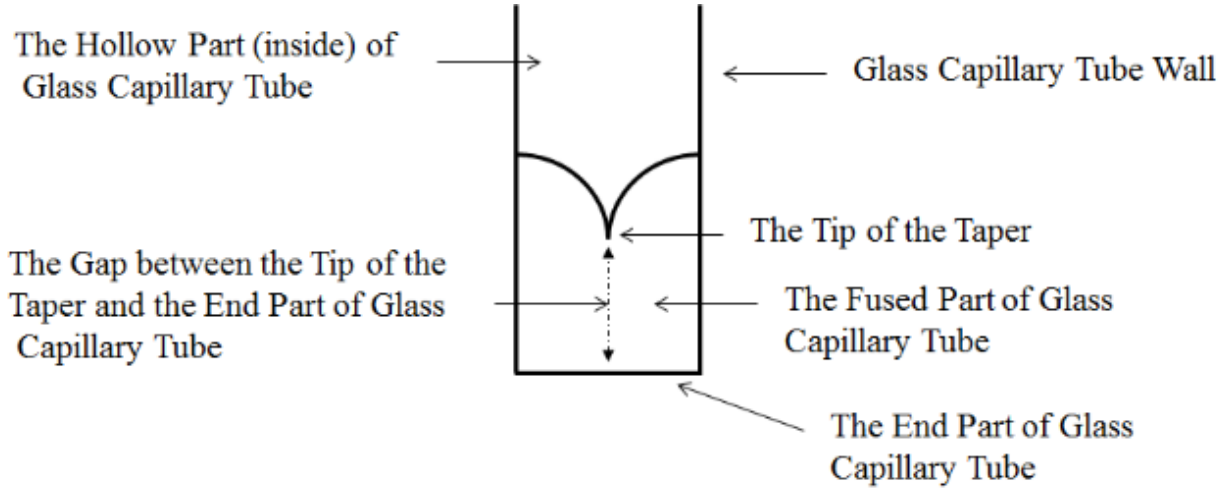
The Hollow Part (inside) of Glass Capillary Tube
Glass Capillary Tube Wall
The Tip of the Taper
The Gap between the Tip of the Taper and the End Part of Glass Capillary Tube
The Fused Part of Glass Capillary Tube
The End Part of Glass Capillary Tube

Figure 2

A

B

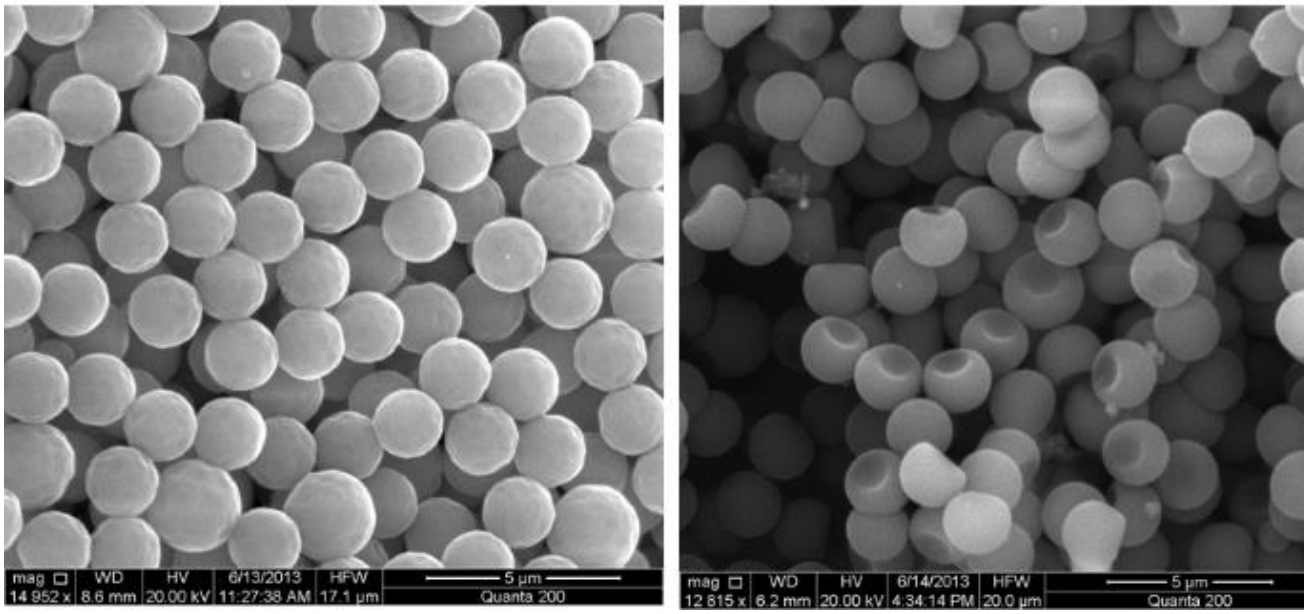
mag
14 952 x
WD
8.6 mm
HV
20.00 kV
6/13/2013
11:27:38 AM
HFW
17.1 µm
5 µm
Quanta 200
mag
12 815 x
WD
8.2 mm
HV
20.00 kV
6/14/2013
4:34:14 PM
HFW
20.0 µm
5 µm
Quanta 200

Figure 3

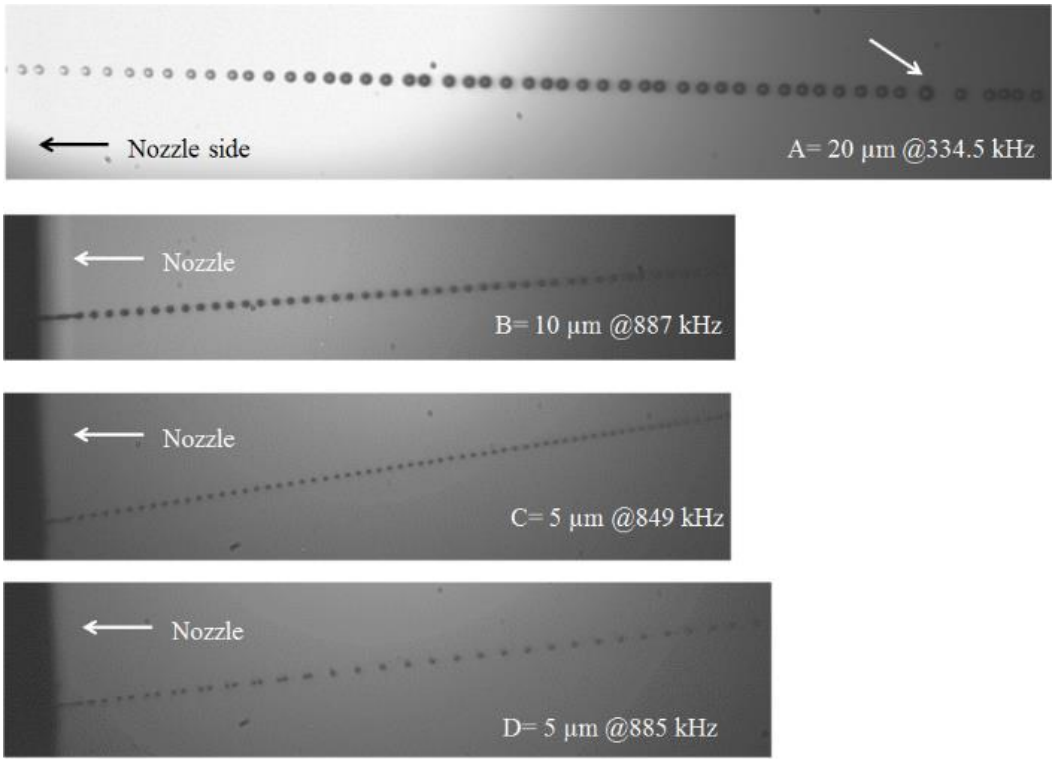
Nozzle side
A= 20 µm @334.5 kHz
Nozzle
B= 10 µm @887 kHz
Nozzle
C= 5 µm @849 kHz
Nozzle
D= 5 µm @885 kHz

Figure 4

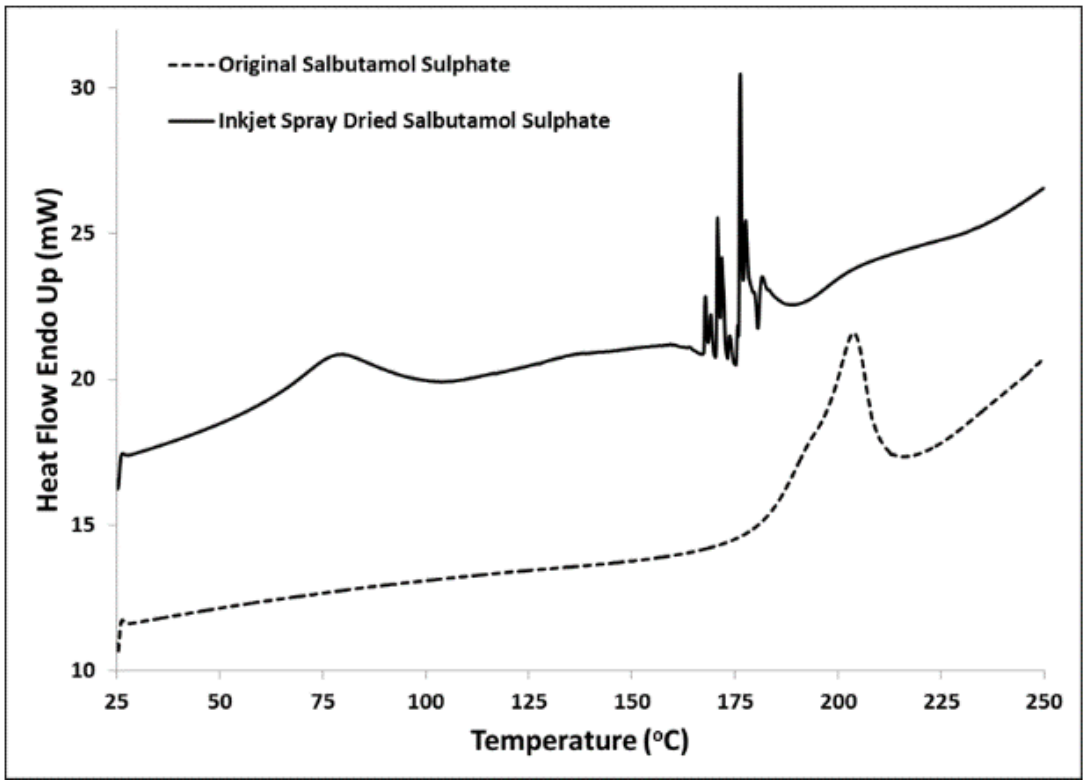
Original Salbutamol Sulphate
Inkjet Spray Dried Salbutamol Sulphate
Heat Flow Endo Up (mW)
30
25
20
15
10
25
50
75
100
125
150
175
200
225
250
Temperature (°C)

Figure 5

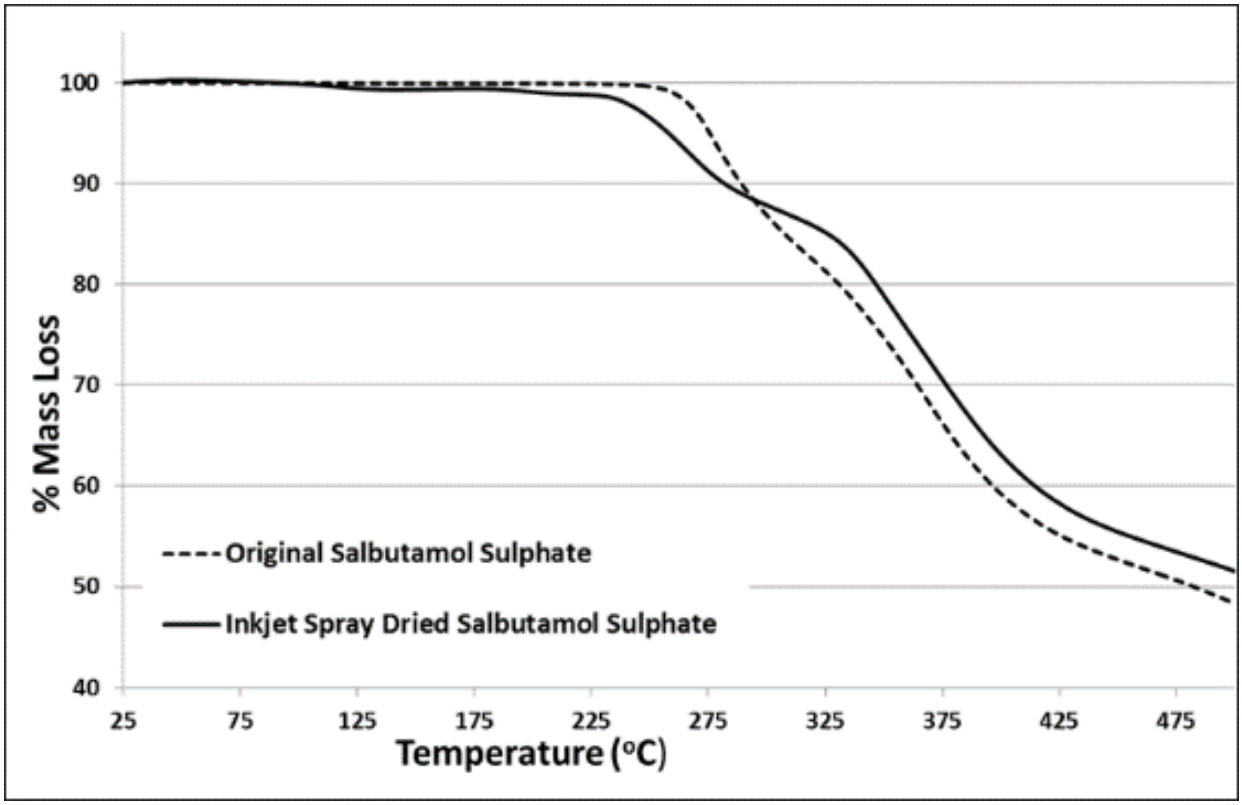
100
90
80
70
60
50
40
% Mass Loss
Original Salbutamol Sulphate
Inkjet Spray Dried Salbutamol Sulphate
25
75
125
175
225
275
325
375
425
475
Temperature (°C)

Figure 6

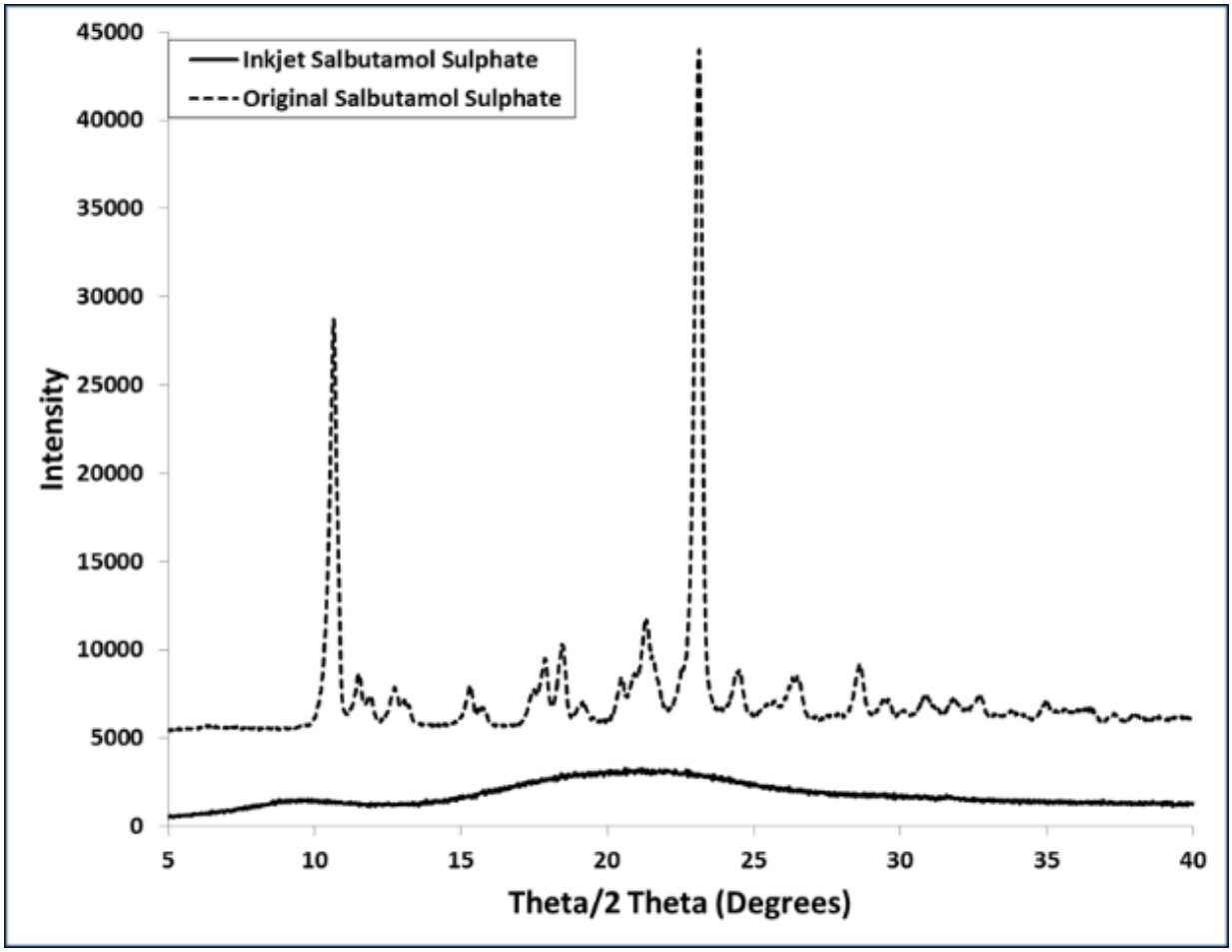
Inkjet Salbutamol Sulphate
Original Salbutamol Sulphate
Intensity
45000
40000
35000
30000
25000
20000
15000
10000
5000
0
5
10
15
20
25
30
35
40
Theta/2 Theta (Degrees)

Figure 7

**Table 1:** Initial configurations of inkjet devices.

| Inkjet device designation | Constriction diameter/ µm | Capsule length/ mm | Orifice diameter/ µm | Piezoelectric disk distance from tip/ mm | Polypropylene tube length /mm | Frequency/ kHz | Current/ A | Driving Voltage V |
|---|---|---|---|---|---|---|---|---|
| A | 60 | 11 | 10 | 1 | 13 | 794 | 0.26 | 30 |
| B | 60 | 11 | 10 | 1 | 13 | 800 | 0.41 | 30 |
| C | 60 | 11 | 10 | 1 | 13 | 362 | 0.26 | 30 |

**Table 2:** Partially optimised configurations of inkjet devices.

| Inkjet device designation | Constriction diameter/ µm | Capsule length/ mm | Orifice diameter/ µm | Piezoelectric disk distance from tip/ mm | Polypropylene tube length /mm | Frequency/ kHz | Current/ A | Driving voltage/ V |
|---|---|---|---|---|---|---|---|---|
| D | 70 | 8 | 10 | 0.5 | 3 | 767.5 | 0.24 | 12 |
| E | 70 | 8 | 10 | 0.5 | 3 | 804.9 | 0.59 | 20 |
| F | 60 | 8 | 10 | 0.5 | 3 | 863.5 | 0.42 | 20 |
| G | 70 | 8 | 5 | 0.5 | 3 | 785.8 | 0.27 | 20 |
| H | 70 | 8 | 5 | 0.5 | 3 | 886.0 | 0.27 | 20 |
| I | 90 | 8 | 5 | 0.5 | 3 | 837.2 | 0.27 | 20 |

**Table 3:** Configurations of inkjet devices with controlled tip geometry.

| Inkjet device designation | Constriction diameter/ µm | Initial tip gap/ µm | Capsule length/ mm | Orifice diameter/ µm | Piezoelectric disk distance from tip/ mm | Polypropylene tube length/ mm | Frequency/ kHz | Current/ A | Driving Voltage/ V | Power consumed per actuation/ µJ |
|---|---|---|---|---|---|---|---|---|---|---|
| J | 70 | 500 | 8 | 10 | 0.5 | 3 | 853.6 | 0.20 | 10 | 2.34 |
| K | 70 | 480 | 7 | 10 | 0.5 | 3 | 914.0 | 0.27 | 20 | 5.91 |
| L | 70 | 380 | 8 | 10 | 0.5 | 3 | 883.3 | 0.27 | 20 | 6.11 |
| M | 80 | 320 | 8 | 5 | 0.5 | 3 | 915.2 | 0.25 | 10 | 2.73 |
| N | 85 | 320 | 9 | 5 | 0.5 | 3 | 824.4 | 0.25 | 10 | 3.03 |
| O | 80 | 410 | 8 | 5 | 0.5 | 3 | 870.1 | 0.22 | 10 | 2.53 |
| P | 30 | 380 | 8 | 5 | 0.5 | 3 | 925.2 | 0.27 | 20 | 5.84 |

**Table 4**: The characteristics of droplets from inkjet devices at high frequencies.

| Orifice diameter (μm) | Frequency (kHz) | Voltage (V) | Current (A) | Drop diameter (μm) | Speed (m/s) | Spacing/diameter |
|---|---|---|---|---|---|---|
| 20 | 334±1 | 13.7 | | 16-19 | 9.5-10 | 1.6-1.8 |
| 10 | 870±1 | 13.7 | 0.27 | 10 | 19±0.2 | 2.1-2.2 |
| 5 | 849 | 20 | 0.27 | 8 | 15 | 2.2 |
| 5 | 855 | 7.6 | 0.22 | 6 | 9 | 1.8 |
| 5 | 885 | 9.8 | 0.22 | 8 | 32 | 5.4 |

**Table 5:** Characterisation of particles made by inkjet devices.

| Inkjet device designation | Orifice diameter (µm) | Drug solution %(w/v) | Particle diameter (µm) (mean ± SD) | GSD | Frequency (kHz) | Feed Rate (ml/hour) |
|---|---|---|---|---|---|---|
| P | 5 | 1 | 1.41 ± 0.13 | 1.09 | 901.4 | 0.76 |
| P | 5 | 3.3 | 2.09 ± 0.14 | 1.06 | 838.6 | 0.46 |
| J | 10 | 1 | 1.95 ± 0.16 | 1.08 | 688.6 | 1.29 |
| K | 10 | 1 | 1.76 ± 0.15 | 1.08 | 903.1 | 1.06 |